THE ASTROPHYSICAL JOURNAL, 231:L97–L100, 1979 July 15

THE ISOTOPIC COMPOSITION OF SOLAR FLARE ACCELERATED NEON

R. A. MEWALDT, J. D. SPALDING, E. C. STONE, AND R. E. VOGT
California Institute of Technology
Received 1979 March 12; accepted 1979 April 6

ABSTRACT

The individual isotopes of neon in energetic solar flare particles have been clearly resolved with a rms mass resolution of 0.20 amu. We find $^{20}Ne/^{22}Ne = 7.6\ (+2.0, -1.8)$ and $^{21}Ne/^{22}Ne \lesssim 0.11$ in the 11–26 MeV per nucleon interval. This isotopic composition is essentially the same as that of meteoritic planetary neon-A and is significantly different from that of the solar wind.

Subject headings: cosmic rays: abundances — solar system: general — Sun: abundances — Sun: flares

I. INTRODUCTION

Energetic solar particle events frequently inject large fluxes of heavy nuclei into the interplanetary medium with energies $\gtrsim$10 MeV per nucleon. High-resolution measurements of the isotopic composition of these nuclei may provide a direct measure of the present solar isotopic makeup, providing crucial information for understanding the history of solar-system material. In addition, such observations are particularly useful for interpreting the integrated effects of solar contributions to other solar-system material. Finally, isotope measurements will add a new dimension to the study of the systematics of solar flare acceleration.

In the case of neon, isotope measurements are available from the solar wind, meteorites, the Earth's atmosphere, and the lunar soil. Because of the diversity of the isotopic compositions observed in these samples, neon is an especially interesting element to study in solar flares.

II. THE INSTRUMENT

The Caltech Heavy Isotope Spectrometer Telescope (HIST) is carried on the *ISEE 3* spacecraft, launched 1978 August 12 into a heliocentric orbit ~0.99 AU from the Sun. HIST is designed to measure the isotopic composition of solar, galactic, and interplanetary cosmic-ray nuclei for the elements Li through Ni in the energy range from ~5 to ~250 MeV per nucleon. A detailed description of the instrument appears in Althouse *et al.* (1978). Briefly, the HIST telescope, shown schematically in Figure 1, consists of an array of solid-state detectors labeled M1, M2, and D1 through D9, the last five having annular guards (G) used as an anticoincidence shield. A unique feature of HIST is the two-dimensional position-sensitive detectors, M1 and M2, which allow the determination of individual particle trajectories. M1 and M2 are 50 μm thick surface barrier devices with a matrix of strips at 1 mm intervals forming an X-Y hodoscope. In addition to identifying the location and number of strips triggered for each analyzed event, the signals from M1 and M2 are analyzed to provide energy-loss information. The energy deposited by particles which stop in detectors M2 through D8 (defined to have range 0 through range 8) is determined in up to five detectors, including the detector in which the particle stops. The present study includes particles stopping in range 2 and range 3.

HIST contains a number of features that allow background rejection and data self-consistency checks not possible in earlier instruments. For example, the trajectory information was used to eliminate events that traverse D1, D2, or D3 within 1 mm of the edge, thereby eliminating possible detector edge effects. We

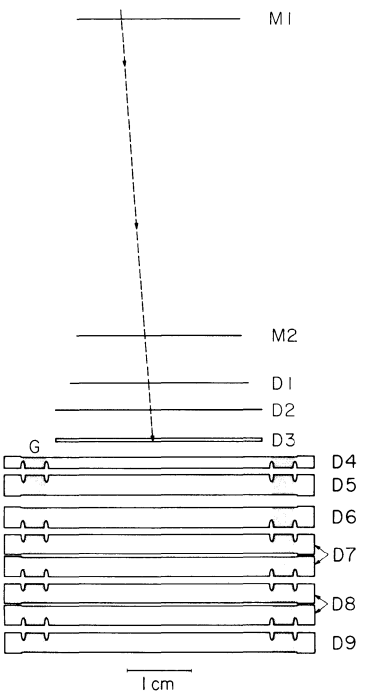

FIG. 1.—Schematic of the HIST sensor. M1, M2, and D1 through D9 are silicon solid-state detectors. The trajectory of a typical range 3 event is indicated.

have also corrected the energy loss in each detector for the particle's trajectory, including the dependence of the detector response on position, as calibrated at the Lawrence Berkeley Laboratory Bevalac. By not considering events where multiple, nonadjacent strips are triggered in M1 or M2, we eliminate essentially all pileup and chance coincidence candidates which could masquerade as heavier rare isotopes.

Resolution of isotopes in HIST is accomplished by a refinement of the standard technique of measuring the particle energy loss ΔE in a detector of thickness L_0 and its residual energy loss E' in a following detector. For example, a particle of mass M, charge Z, and kinetic energy E has a range approximated by

$$R = k\frac{M}{Z^2}\left(\frac{E}{M}\right)^a.$$

Combining this with a similar equation for the residual range $R - L$ of the particle after traversing a path length $L = L_0 \sec\theta$ at angle θ, we find

$$M = \left[\frac{k(\Delta E + E')^a - kE'^a}{Z^2 L_0 \sec\theta}\right]^{1/(a-1)}. \quad (1)$$

Isotope resolution, then, depends on precise measurements of the energy losses ΔE and E', the path length L, and an accurate range-energy relation. For the preliminary report in this *Letter*, we have used a range-energy relation for heavy ions from Barkas and Berger (1964) modified by small empirical correction factors. The response of HIST to isotopes with $3 \leq Z \leq 26$ has been calibrated at the Bevalac and this information has been used to confirm that the dominant neon isotope is ^{20}Ne.

III. THE OBSERVATIONS

On 1978 September 23, a large solar particle event was detected by HIST and by ground-level neutron monitors within 1 hour after the observation of a 2B Hα solar flare at 35° N, 50° W (*Solar Geophysical Data Bulletin*, 1978 October, November). The neon data included in this study were obtained from 10:00 UT on 1978 September 23 to 23:59 UT on 1978 September 27, during which more than 10^4 particles with $Z \geq 6$ were analyzed.

For each stopping particle which triggers N detectors it is possible to make $N - 1$ determinations of Z and M by appropriate choices of the detectors in which to measure ΔE versus E' for use in equation (1). Comparison of these determinations is a powerful technique for identifying background events. Figure 2 shows a cross plot of M_{23} (determined from D2 versus D3) versus M_{13} (determined from D1 versus D2 + D3) for range 3 neon events. Note the concentration of events at the ^{20}Ne intersection, with a smaller grouping at ^{22}Ne. The events for which M_{23} does not agree well with M_{13} can be eliminated by placing requirements on the consistency between M_{23} and M_{13}, as indicated in Figure 2. For range 2 events we computed three masses: M_{12} (based on D1 versus D2); M_{B2} (based on M2 versus D1 + D2); and M_{A2} (based on M1 versus M2+D1+D2). We then accepted for further analysis

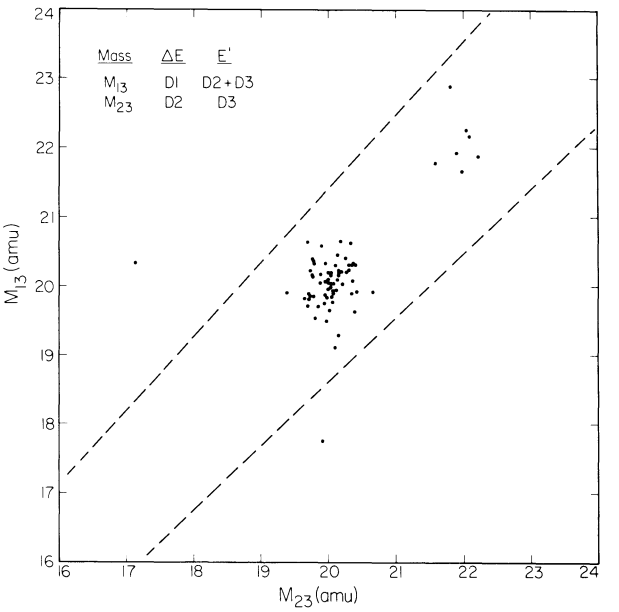

FIG. 2.—Comparison of mass measurements for range 3 neon events. Events outside the dashed lines were rejected.

only those events for which M_{A2} and M_{B2} were consistent with M_{12} to within $\pm 7\%$.

For the accepted events, a best estimate of M was computed from a weighted average of the individual mass determinations, using weighting factors derived from the observed resolution for ^{16}O events. Figure 3 shows the resulting histograms of M, where we note well-separated peaks due to ^{20}Ne and ^{22}Ne, with no evidence of any ^{21}Ne. The observed mass resolution σ is 0.20 amu for both ranges. These are the first measurements in which individual solar flare isotopes with $Z > 2$ have been resolved.

Because the instrument selects events for analysis on the basis of range, the energy per nucleon intervals for ^{20}Ne and ^{22}Ne differ slightly. We have corrected for this difference, using the observed energy spectrum of ^{20}Ne. For energies from 11 to 26 MeV per nucleon, we find $^{20}\text{Ne}/^{22}\text{Ne} = 7.6$ $(+2.0, -1.8)$ and an 84% confidence level upper limit of $^{21}\text{Ne}/^{22}\text{Ne} < 0.11$.

We have considered whether our neon observations might include spallation contributions arising from the passage of flare particles through the solar atmosphere. At 11–26 MeV per nucleon the prompt production of ^{21}Ne is dominated by $^{22}\text{Ne}(p, d)^{21}\text{Ne}$ and $^{24}\text{Mg}(p, \alpha)^{21}\text{Na}$, where ^{21}Na decays to ^{21}Ne with a half-life of 22.8 s. Prompt ^{22}Ne is produced mainly by $^{23}\text{Na}(p, 2p)^{22}\text{Ne}$. For a nominal solar atmospheric composition, ^{21}Ne production should be significantly greater than ^{22}Ne, and thus the absence of observed ^{21}Ne implies that less than one ^{22}Ne event could be expected in our data from production by spallation at the time of the flare. Furthermore, from the absence of ^{21}Ne relative to ^{24}Mg in our observations, we infer that the path length of accelerated flare particles in the solar atmosphere was <0.2 g cm^{-2}.

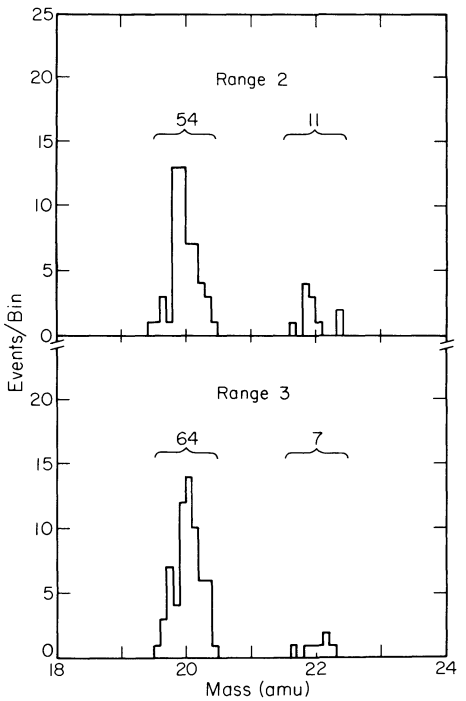

FIG. 3.—Mass histograms of range 2 and range 3 neon events. The ^{22}Ne energy intervals are 11–15 and 15–26 MeV per nucleon, while those for ^{20}Ne are ~6% higher.

IV. DISCUSSION

There are two previous direct measurements of neon isotopes from the Sun. Geiss and collaborators have measured directly the elemental and isotopic compositions of solar wind He, Ne, and Ar during the *Apollo* lunar landings. They found average abundances of $^{20}Ne/^{22}Ne = 13.7 \pm 0.3$ and $^{21}Ne/^{22}Ne = 0.033 \pm 0.004$ (Geiss 1973). Dietrich and Simpson (1978) have reported an average value for the $^{20}Ne/^{22}Ne$ ratio at 28–50 MeV per nucleon, summed over seven large solar flares. Using least-squares fitting techniques, they found $^{20}Ne/^{22}Ne = 7.0\ (+2.3, -1.5)$, consistent with our measurement, and significantly lower than the solar wind $^{20}Ne/^{22}Ne$ ratio. With our improved resolution, a maximum likelihood calculation indicates that there is only a 1% probability that our observations are consistent with a $^{20}Ne/^{22}Ne$ ratio as large as that of the solar wind.

If the neon isotopic compositions of the solar wind and solar flares are indeed significantly different, one must ask whether either reflects the composition of the Sun. Recent observations have shown that the *elemental* composition of solar flares is highly variable, and, when normalized to oxygen, frequently enriched in nuclei with $Z > 8$ relative to the solar photospheric or coronal composition (see, e.g., Crawford *et al.* 1975). However, these elemental enhancements probably depend on atomic rather than nuclear phenomena (see, e.g., Webber 1975), and therefore relative isotopic abundances might be preserved in the acceleration process.

Helium is the only element for which the solar flare isotopic composition has been studied in detail. In many flares ^{3}He is enhanced orders of magnitude above its solar abundance, including occasional typically small flare events with $^3He/^4He \sim 1$ (see, e.g., Ramaty *et al.* 1978). Fisk (1978) has recently suggested a plasma mechanism that may preferentially heat and therefore enhance ambient ^{3}He in small flares. This mechanism might also enhance heavy elements, but its effect for heavier nuclei, which have a multiplicity of possible ionization states, would probably depend only weakly on the nuclide's mass.

Although heavy elements in the solar wind have not been studied to the extent that they have been in solar flares, time variations have been observed in the He/H and He/O elemental ratios and the $^3He/^4He$ isotopic ratio (Bame 1972), and therefore selective acceleration may be important. A modest (~10%) depletion of ^{22}Ne relative to ^{20}Ne might be expected during solar wind acceleration on the basis of one model (Geiss 1972). It is possible, however, that the actual ^{22}Ne depletion in the solar wind is larger.

Isotope measurements of neon are also available from other solar-system material, including meteorites, the lunar soil, and the Earth's atmosphere (see, e.g., the review by Podosek 1978). In meteorites, the elemental abundances of trapped noble gases occur in two characteristic patterns which Signer and Suess (1963) designated *solar* and *planetary*. Solar noble gas is characterized by a modest enrichment in the heavier noble gases relative to those in the Sun, while in planetary noble gas, the heavier gases are systematically enriched by up to several orders of magnitude.

Solar and planetary gases also differ in isotopic structure. Meteoritic measurements of neon indicate three major isotopically distinct components, including the planetary component neon-A with $^{20}Ne/^{22}Ne \approx 8.2$, and the solar component neon-B, with $^{20}Ne/^{22}Ne \approx 12.5$ (Pepin 1967). Figure 4 shows these two *trapped* components in a conventional three-isotope diagram, along with the *spallation* component (labeled *S* in the Fig. 4 inset), which consists of roughly equal parts of ^{20}Ne, ^{21}Ne, and ^{22}Ne created in situ by cosmic-ray spallation of meteoritic material. Because of the similarity of the $^{20}Ne/^{22}Ne$ ratios in neon-B and the solar wind (see Fig. 4), neon-B is generally regarded to be the result of the direct implantation of solar wind neon into meteoritic material. A similar component is found in lunar samples. In the "single component" view, neon-B is primordial, and compositions that are richer in ^{22}Ne are generated by fractionation processes, such as preferential diffusive loss of ^{20}Ne (Zahringer 1964). The evidence now favors a multicomponent viewpoint (e.g., Black 1972*a*, *b*), in which compositions along the line AB in the Figure 4 inset result from mixing a neon-A and neon-B. Note in Figure 4 that our observation of solar flare nuclei is consistent with neon-A, but not with neon-B.

Also shown in Figure 4 are additional, less prominent

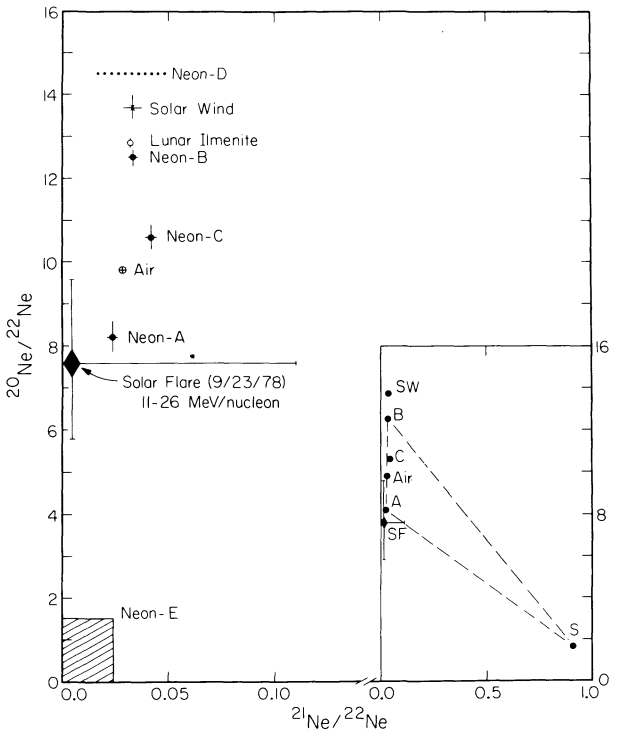

FIG. 4.—A comparison of various solar-system isotope measurements of neon based on similar compilations by Podosek (1978) and Eberhardt (1978). In addition, Dietrich and Simpson (1978) have reported a seven-flare average value of $^{20}Ne/^{22}Ne = 7.0$ $(+2.3, -1.5)$, with no indication of the $^{21}Ne/^{22}Ne$ ratio. The inset shows selected compositions on a different scale, including the cosmic-ray spallation component *S*. Meteoritic neon compositions generally fall within the triangle BAS.

meteoritic components (neon-C, neon-D, and neon-E) as identified by Black (1972*a*,*b*). Of particular interest here is neon-C, which Black attributed to the direct implantation of solar cosmic rays (however, see also Walton *et al.* 1974). Note that the two direct measurements of solar cosmic rays are only marginally consistent with neon-C.

Although a conclusive identification of our measurement with the meteoritic components is not at present possible, the comparison of the solar flare and solar wind compositions provides direct support for multicomponent views of neon isotopic structures in the solar system in that at least two isotopically distinct components appear to be now emitted by the Sun. It is possible that the isotopic composition of neon in the Sun is the same as that of the "planetary" component neon-A, and isotopic differentiation associated with solar wind acceleration results in the enhanced $^{20}Ne/^{22}Ne$ ratio which is characteristic of neon-B. Measurements of the isotopic composition of several other elements with $Z \geq 6$, which will soon be available from analysis of additional HIST data, should allow limits to be placed on the extent of any mass-dependent selection effects in solar flare acceleration, so that solar flare observations can be related directly to the isotopic composition of the Sun.

W. E. Althouse, A. C. Cummings, and T. L. Garrard made significant contributions to the design and development of the HIST instrument. This work was supported in part by NASA under contract NAS5-20721 and grant NGR 05-002-160.

REFERENCES

Althouse, W. E., Cummings, A. C., Garrard, T. L., Mewaldt, R. A., Stone, E. C., and Vogt, R. E. 1978, *Geosci. Electronics*, **16**, 204.
Bame, S. J. 1972, in *Solar Wind*, ed. C. P. Sonnett, P. J. Coleman, Jr., and J. M. Wilcox (NASA SP-308), p. 535.
Barkas, W. H., and Berger, M. J. 1964, NASA SP-3013.
Black, D. C. 1972*a*, *Geochim. Cosmochim. Acta*, **36**, 347.
———. 1972*b*, *Geochim. Cosmochim. Acta*, **36**, 377.
Crawford, H. J., Price, P. B., Cartwright, B. G., and Sullivan, J. D. 1975, *Ap. J.*, **195**, 213.
Dietrich, W. F., and Simpson, J. A. 1978, talk, American Physical Society Topical Conference on Cosmic Ray Astrophysics, Durham, NH.
Eberhardt, P. 1978, *Geochim. Cosmochim. Acta Suppl.*, in press.
Fisk, L. A. 1978, *Ap. J.*, **224**, 1048.
Geiss, J. 1972, in *Solar Wind*, ed. C. P. Sonnett, P. J. Coleman, Jr., and J. M. Wilcox (NASA SP-308), p. 559.
———. 1973, *13th Internat. Cosmic Ray Conf.* (Denver: University of Denver), **5**, 3375.
Pepin, R. O. 1967, *Earth Planet. Sci. Letters*, **2**, 13.
Podosek, F. A. 1978, *Ann. Rev. Astr. Ap.*, **16**, 293.
Ramaty, R., *et al.* 1978, NASA TM 79660.
Signer, P., and Suess, H. E. 1963, in *Earth Science and Meteorites*, ed. J. Geiss and E. D. Goldberg (Amsterdam: North-Holland), p. 241.
Walton, J. R., Heymann, D., Jordan, J. L., and Yaniv, A. 1974, *Geochim. Cosmochim. Acta Suppl.*, **5**, 2045.
Webber, W. R. 1975, *14th Internat. Cosmic Ray Conf.* (Munich: Max-Planck-Institut für extraterrestrische Physik), **5**, 1597.
Zahringer, J. 1964, *Ann. Rev. Astr. Ap.*, **2**, 121.

R. A. MEWALDT, J. D. SPALDING, E. C. STONE, and R. E. VOGT: California Institute of Technology, George W. Downs Laboratory of Physics, Pasadena, CA 91125